

## **Supporting Information**

# **Ultrathin Two-dimensional-BiOCl with Oxygen Vacancies Anchored in Three-dimensional-Porous g-C<sub>3</sub>N<sub>4</sub> to Construct a Hierarchical Z-Scheme Heterojunction for Photocatalytic Degradation of NO**

*Mengmeng Wang, Beibei Wang, Bingke Xie, Najun Li, Qingfeng Xu, Hua Li, Jinghui He, Dongyun Chen,\* and Jianmei Lu\**

College of Chemistry, Chemical Engineering and Materials Science, Collaborative Innovation Center of Suzhou Nano Science and Technology, Soochow University, Suzhou 215123, China

### **Corresponding Author**

\*Dongyun Chen. E-mail: [dychen@suda.edu.cn](mailto:dychen@suda.edu.cn)

\*Jianmei Lu. E-mail: [lujm@suda.edu.cn](mailto:lujm@suda.edu.cn).

## **Table of Contents**

**S1. XRD spectra and FTIR spectra**

**S2. EIS spectra**

**S3. Table S1. Data comparison of photocatalytic NO removal over different catalysts**

**S4. XRD spectra of 30% BCO/CNS-15 before and after cycling**

**S5. XPS spectra and TEM image of 30% BCO/CNS-15 after photoreaction**

**S6. The amount of by-product NO<sub>2</sub> produced during irradiation**

**S7. The specific peak content ratio of the fitted data of Bi 4f in XPS**

**S8. References**

### S1. XRD spectra and FTIR spectra

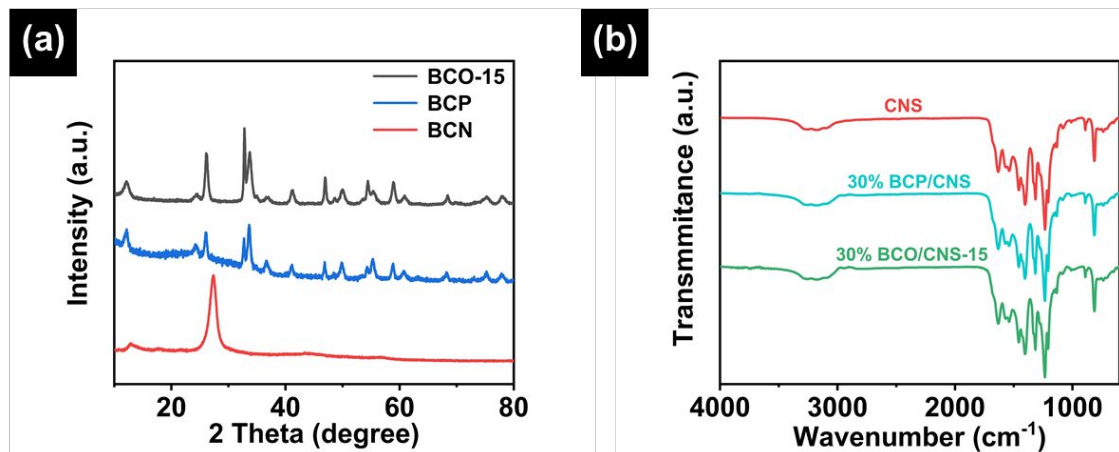


**Figure S1.** (a) XRD spectra of BCO-15, BCP and BCN, (b) FTIR spectra of CNS, 30% BCP/CNS and 30% BCO/CNS-15.

### S2. EIS spectra

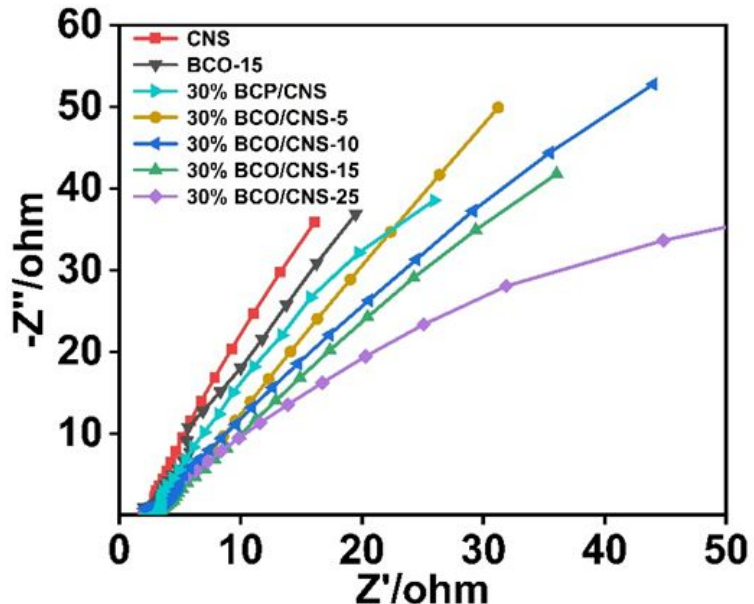


**Figure S2.** EIS spectra of the synthesized photocatalysts.

**S3. Table S1. Data comparison of photocatalytic NO removal over different catalysts.**

Catalyst	Catalyst	NO (mg)	Light type (ppb)	Time (Xe lamp) (min)	$\eta$ (%)	Ref
Ag NCs/TiO <sub>2</sub>	50	600	300 W	30	62.0	[1]
Ag-TiO <sub>2-x</sub>	50	450	300 W	20	44.3	[2]
Bi <sub>2</sub> O <sub>2</sub> CO <sub>3</sub> -g-C <sub>3</sub> N <sub>4</sub>	100	400	300 W	30	34.8	[3]
20-Bi/BiOI	50	500	500 W	30	32	[4]
Bi-g-C <sub>3</sub> N <sub>4</sub>	200	500	150 W	30	60.8	[5]
O-ACN-Ba	200	500	150 W	30	50.4	[6]
BOC/BOB	108	430	300 W	30	53.2	[7]
LaFeO <sub>3</sub> -SrTiO <sub>3</sub>	100	600	300 W	30	45	[8]
Cu <sup>2+</sup> /g-C <sub>3</sub> N <sub>4</sub>	50	600	300 W	30	51	[9]
CN-KCl-3%	200	600	300 W	30	53.1	[10]
BiOCl/PPy	200	600	300 W	30	34.1	[11]
BiOBr-3C	100	600	300 W	30	28.0	[12]
CQDs/ZnFe <sub>2</sub> O <sub>4</sub>	200	600	150 w	30	38.7	[13]
Bi/BiOI	50	500	500 W	60	46.5	[14]

---

30% BCO/CNS-15      100      600      300 W      30      66.5      This work

---

**S4. XRD spectra of 30% BCO/CNS-15 before and after cycling**

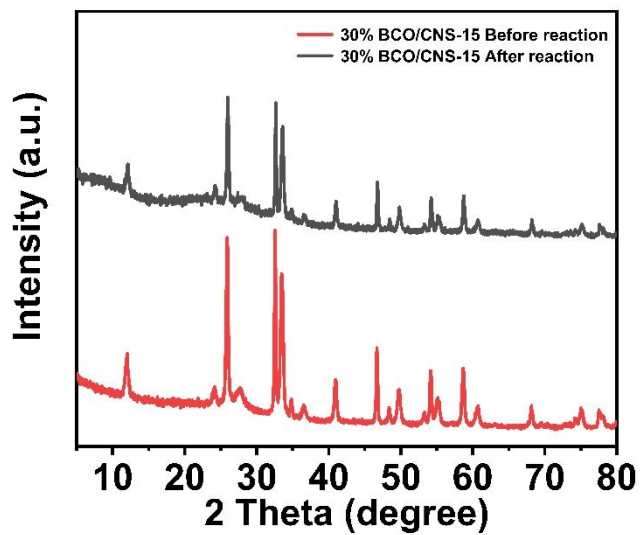


**Figure S4.** XRD spectra of 30% BCO/CNS-15 before and after cycling.

**S5. XPS spectra and TEM image of 30% BCO/CNS-15 after photoreaction**

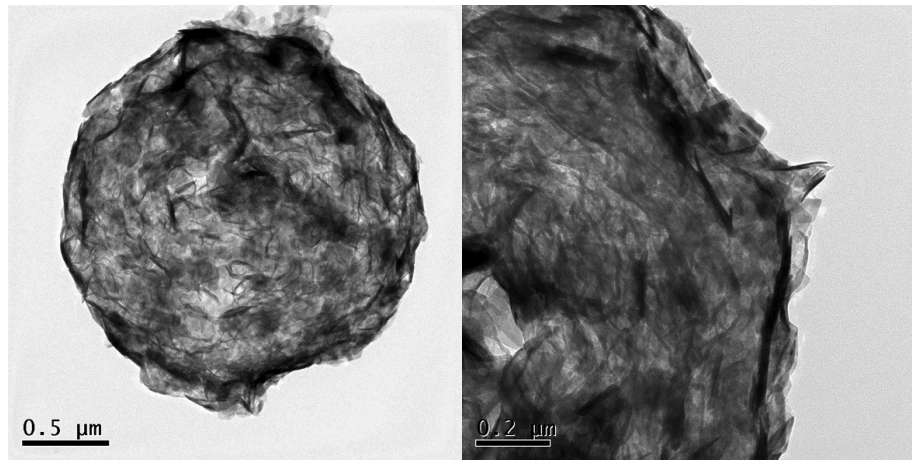


**Figure S5.** TEM images of 30% BCO/CNS-15 after photoreaction.

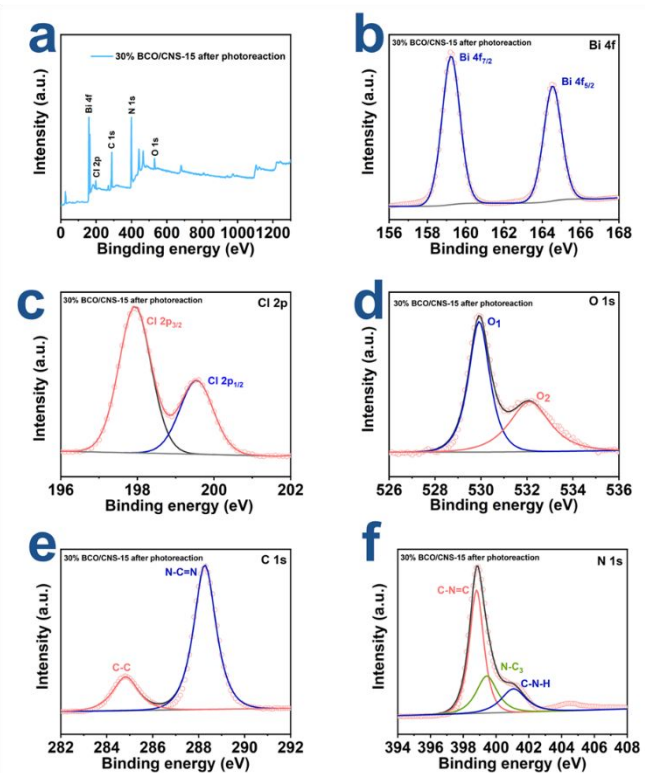


**Figure S6.** XPS (a) survey scan and high-resolution spectra of (b) Bi 4f, (c) Cl 2p, (d) O 1s, (e) C 1s, and (f) N 1s of 30% BCO/CNS-15 after photoreaction.

**S6. The amount of by-product NO<sub>2</sub> produced during irradiation**

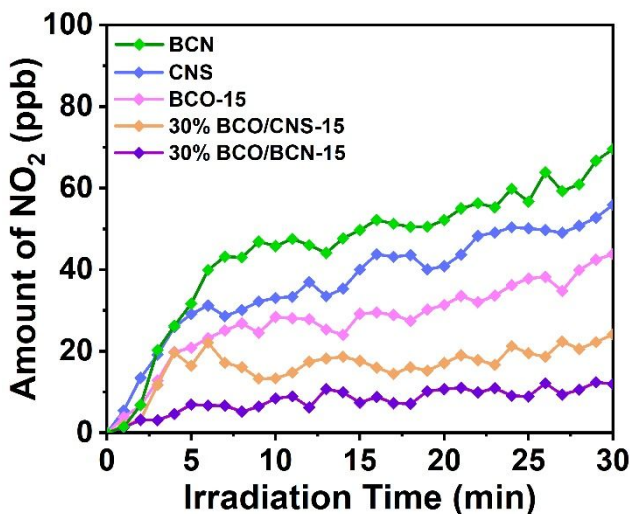


**Figure S7.** The amount of by-product NO<sub>2</sub> produced during irradiation.

### S7. The specific peak content ratio of the fitted data of Bi 4f in XPS

**Table S2. Data comparison of specific peak content ratio of the fitted data of Bi 4f in XPS over BCO-15 and 30% BCO/CNS-15 catalysts.**

Catalysts	Bi <sup>(3-x)+</sup>	Bi <sup>3+</sup>
<b>BCO-15</b>	<b>46.78%</b>	<b>53.22%</b>
<b>30% BCO/CNS-15</b>	<b>58.97%</b>	<b>41.03%</b>

### S8. References:

- [1] Duan, Y.; Luo, J.; Zhou, S.; Mao, X.; Shah, M. W.; Wang, F.; Chen, Z.; Wang, C. TiO<sub>2</sub>-supported Ag nanoclusters with enhanced visible light activity for the photocatalytic removal of NO. *Appl. Catal. B* **2018**, *234*, 206-212.
- [2] Duan, Y.; Zhang, M.; Wang, L.; Wang, F.; Yang, L.; Li, X.; Wang, C. Plasmonic Ag-TiO<sub>2-x</sub> nanocomposites for the photocatalytic removal of NO under visible light with high selectivity: The role of oxygen vacancies. *Appl. Catal. B* **2017**, *204*, 67-77.
- [3] Wang, Z.; Huang, Y.; Ho, W.; Cao, J.; Shen, Z.; Lee, S. C. Fabrication of Bi<sub>2</sub>O<sub>2</sub>CO<sub>3</sub>/g-C<sub>3</sub>N<sub>4</sub> heterojunctions for efficiently photocatalytic NO in air removal: In-situ self-sacrificial synthesis, characterizations and mechanistic study. *Appl. Catal. B* **2016**, *199*, 123-133.
- [4] Li, Q.; Gao, S.; Hu, J.; Wang, H.; Wu, Z. Superior NO<sub>x</sub> photocatalytic removal over

- hybrid hierarchical Bi/BiOI with high non-NO<sub>2</sub> selectivity: synergistic effect of oxygen vacancies and bismuth nanoparticles. *Catal. Sci. Technol.* **2018**, *8*, 5270-5279.
- [5] Jiang, G.; Li, X.; Lan, M.; Shen, T.; Lv, X.; Dong, F.; Zhang, S. Monodisperse bismuth nanoparticles decorated graphitic carbon nitride: Enhanced visible-light-response photocatalytic NO removal and reaction pathway. *Appl. Catal. B* **2017**, *205*, 532-540.
- [6] Cui, W.; Li, J.; Sun, Y.; Wang, H.; Jiang, G.; Lee, S. C.; Dong, F. Enhancing ROS generation and suppressing toxic intermediate production in photocatalytic NO oxidation on O/Ba co-functionalized amorphous carbon nitride. *Appl. Catal. B* **2018**, *237*, 938-946.
- [7] Zhu, G.; Li, S.; Gao, J.; Zhang, F.; Liu, C.; Wang, Q.; Hojamberdiev, M. Constructing a 2D/2D Bi<sub>2</sub>O<sub>2</sub>CO<sub>3</sub>/Bi<sub>4</sub>O<sub>5</sub>Br<sub>2</sub> heterostructure as a direct Z-scheme photocatalyst with enhanced photocatalytic activity for NO<sub>x</sub> removal. *Appl. Surf. Sci.* **2019**, *493*, 913-925.
- [8] Zhang, Q.; Huang, Y.; Peng, S.; Zhang, Y.; Shen, Z.; Cao, J.-j.; Ho, W.; Lee, S. C.; Pui, D. Y. H. Perovskite LaFeO<sub>3</sub>-SrTiO<sub>3</sub> composite for synergistically enhanced NO removal under visible light excitation. *Appl. Catal. B* **2017**, *204*, 346-357.
- [9] Zhao, L.; Dong, G.; Zhang, L.; Lu, Y.; Huang, Y. Photocatalytic Nitrogen Oxide Removal Activity Improved Step-by-Step through Serial Multistep Cu Modifications. *ACS Appl. Mater. Interfaces.* **2019**, *11*, 10042-10051.
- [10] Xiong, T.; Wang, H.; Zhou, Y.; Sun, Y.; Cen, W.; Huang, H.; Zhang, Y.; Dong, F. KCl-mediated dual electronic channels in layered g-C<sub>3</sub>N<sub>4</sub> for enhanced visible light photocatalytic NO removal. *Nanoscale* **2018**, *10*, 8066-8074.
- [11] Zhao, Z.; Cao, Y.; Dong, F.; Wu, F.; Li, B.; Zhang, Q.; Zhou, Y. The activation of oxygen through oxygen vacancies in BiOCl/PPy to inhibit toxic intermediates and enhance the activity of photocatalytic nitric oxide removal. *Nanoscale* **2019**, *11*, 6360-6367.
- [12] Liao, J.; Chen, L.; Sun, M.; Lei, B.; Zeng, X.; Sun, Y.; Dong, F. Improving visible-light-driven photocatalytic NO oxidation over BiOBr nanoplates through tunable oxygen vacancies. *Chin. J. Catal.* **2018**, *39*, 779-789.
- [13] Huang, Y.; Liang, Y.; Rao, Y. Environment-Friendly Carbon Quantum Dots/ZnFe<sub>2</sub>O<sub>4</sub> Photocatalysts: Characterization, Biocompatibility, and Mechanisms for NO Removal. *Environ. Sci. Technol.* **2017**, *51*, 2924-2933.

[14] Li, Q.; Gao, S.; Hu, J.; Wang, H.; Wu, Z. Superior NO<sub>x</sub> photocatalytic removal over hybrid hierarchical Bi/BiOI with high non-NO<sub>2</sub> selectivity: synergistic effect of oxygen vacancies and bismuth nanoparticles. *Catal. Sci. Technol.* **2018**, *8*, 5270-5279.